JOURNAL OF CHEMICAL & ENGINEERING DATA

ARTICLE

pubs.acs.org/jced

Water Dispersibility and Temperature Dependence of Electrical Conductivity of Conductive Polypyrrole Nanoparticles Doped with Fulvic Acids

Chao Yang and Peng Liu*

State Key Laboratory of Applied Organic Chemistry and Institute of Polymer Science and Engineering, College of Chemistry and Chemical Engineering, Lanzhou University, Lanzhou 730000, China

ABSTRACT: The water-dispersed conductive polypyrrole (PPy) nanoparticles were prepared via the chemical oxidative polymerization with fulvic acids (FAs), a renewable resource from both soils and municipal waste compost, as dopant and stabilizer for tuning the properties of polypyrrole nanoparticles. The FA-doped polypyrrole (PPy/FAs) nanoparticles were characterized with Fourier transform infrared (FTIR), UV−vis, thermogravimetric analysis (TGA), transmission electron microscopy (TEM), and electric conductivity. The diameters of the PPy/FAs nanoparticles decreased from (150 to 20) nm with the increasing of the feeding ratio of FAs, and the PPy/FAs nanoparticles could be well-dispersed in water. Their electrical conductivities were affected markedly by the amount of the natural dopant added. They have weakly temperature-dependent conductivity over the entire temperature interval from (283 to 423) K.

INTRODUCTION

Conducting electroactive polymers (CEP) remain a subject of intense investigation of many research groups worldwide. Polypyrrole (PPy) is one of the most widely investigated conducting polymers because of its good thermal and environmental stability and good electrical conductivity, which are favorable for various applications such as metallization of dielectrics,[1] batteries,[2] antistatic coatings,[3] shielding of electromagnetic interferences,[4] sensors,[5] actuators,[6] microactuators,[7] etc.

Most recently, the natural products and their derivatives, such as lignin and cellulose, have attracted more and more attention as the dopants and/or stabilizers in the in situ doping polymerization to afford PPy with high conductivity, good solubility, and special morphology due to their biocompatibility and biodegradation.[8,9]

Fulvic acids (FAs) (Figure 1),[10] a specific class of dissolved humic substances found in the hydrosphere, are one of the most significant renewable resources and constituents of organic matter in both soils and municipal waste compost and have a relevant role in the cycling of many elements in the environment and in soil ecological functions.[11] They contain about 10 % less carbon and 10 % more oxygen than humic acids and have more than double the content of carboxylic acid groups.[12] They were also used to control the size and shape of gold nanoparticles[13] and stabilize the single-walled carbon nanotubes[14] except in the environmental science. Because of their plentiful carboxyl and hydroxyl groups, they are expected to be potential dopants and stabilizers for the conducting polymers. However, there is no correlative work reported up to now.

In the present work, the FAs were used as both the stabilizer (or template) and the dopant for the chemical oxidative polymerization of pyrrole. The effect of FAs on the morphology, water dispersibility, and electrical conductivity of the products was investigated.

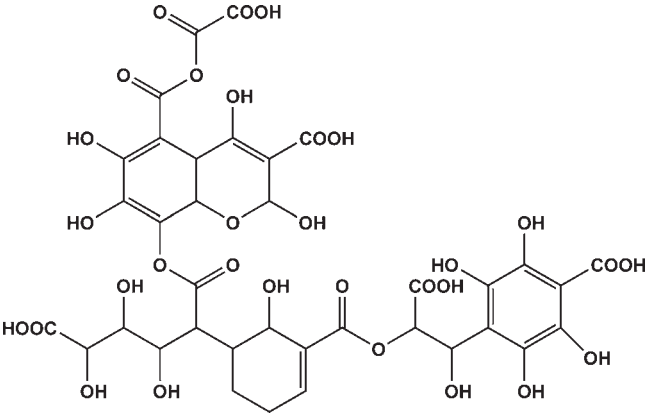

Figure 1. Typical proposed formula of FAs.

EXPERIMENTAL SECTION

Materials. The pyrrole monomer (Acros Organics), after being dehydrated with calcium hydride for 24 h, was distilled under reduced pressure before use. Ammonium peroxodisulfate (APS) (Tianjin Chemical Reagent Co., Tianjin, China) was used as an oxidant, and fulvic acids which were purchased from the Tongwei Biotechnology Co. Ltd. (>0.95 mass fraction, Shanghai, China) were used as dopant and stabilizer as received. Ethanol was of analytical grade and used without further purification. Doubly deionized water was used through all the processes.

Chemical Synthesis. Fulvic acid was added to 100 mL of double distilled water in a 250 mL round-bottom flask and stirred

Special Issue: John M. Prausnitz Festschrift

Received: July 17, 2010
Accepted: September 10, 2010
Published: September 23, 2010

Table 1. Emulsion Polymerizing Conditions

sample	Py (mL)	FAs (g)	APS (g)
S-1	1	0.01	0.9
S-2	1	0.05	0.9
S-3	1	0.10	0.9
S-4	1	0.24	0.9
S-5	1	0.42	0.9
S-6	1	0.97	0.9
S-7	1	2.26	0.9

for 15 min. Freshly distilled pyrrole (1.0 mL, 0.0144 mol) was added to the above solution, and the mixture was stirred for 45 min in ice-cold conditions to obtain a white-turbid mixture. The conditions of the polymerizations are given in Table 1. Ammonium peroxodisulfate (0.9 g, 0.015 mol) in 10 mL of double distilled water was added drop by drop to the above solution, and stirring was continued for 10 h under ice-cold conditions. The resulting polypyrrole was purified by being poured into a large excess of distilled water, filtered, and washed with distilled water and ethanol until the filtrate became colorless. The black powder samples were dried under vacuum (0.1 mm of Hg) for 24 h prior to further analysis.

Characterizations. The FTIR measurements (Impact 400, Nicolet, Waltham, MA) were carried out with the KBr pellet method. Thermogravimetric results were obtained with a TA Instrument 2050 thermogravimetric analyzer at a heating rate of 10 °C·min^{-1} from (25 to 800) °C under a nitrogen atmosphere. Electronic absorption spectra of the PPy/FAs samples were recorded in water solution in the wavelength range of (200 to 1200) nm at room temperature by using a Lambda 35 UV−vis spectrometer (PerkinElmer, U.S.A.). The morphologies of the PPy/FAs samples were characterized with a JEM-1200 EX/S transmission electron microscope (TEM) (JEOL, Tokyo, Japan). The powders were dispersed in water in an ultrasonic bath for 30 min and then deposited on a copper grid covered with a perforated carbon film.

The electrical conductivities of the PPy powders were measured using a SDY-4 Four-Point ProbeMeter (Guangzhou Semiconductor Material Academe) at ambient temperature employing the method on a pressed pallet according to the formula

$$\sigma = 1/\rho = V/I = F(D/S)\cdot F(W/S)\cdot W\cdot F_{sp}$$

where σ referred to electrical conductivity, V the voltage, I the current, D the diameter of the pallets, W the thickness of the pallets, S the average space between of the probes, $F(D/S)$ the amendatory coefficient of the diameter of the pallets, $F(W/S)$ the amendatory coefficient of the thickness of the pallets, and F_{sp} the amendatory coefficient of the space between the probes. The pellets were obtained by subjecting the powder sample to a pressure of 30 MPa. The reproducibility of the result was checked by measuring the resistance three times for each pallet.

The temperature dependence of conductivity was determined by a WDJ-1 KH Variable-Temperature Resistance Measuring Instrument (Institute of Chemistry, the Chinese Academy of Sciences) at a heating rate of 5 °C·min^{-1} from (25 to 150) °C.

RESULTS AND DISCUSSION

Morphological and Dispersion Stability. The TEM images of the PPy/FAs samples dispersed in water were given in Figure 2. The PPy/FAs sample S-1 appeared to be a cluster of jumbled particles and could not be dispersed. With increasing FA feeding ratio, the morphologies of the PPy/FAs particles became smaller, and their dispersibility in water was improved consequently. TEM images of the samples clearly indicate that the products are uniform solid nanoparticles, and their diameters are about (200, 100, and 20) nm for samples S-3, S-5, and S-7, respectively. It indicated that the FA molecules acted as the template (or stabilizer) as well as the dopant, as reported previously.[9]

This might be due to the excessive FAs which interact with PPy through the formation of hydrogen bonds to play the role as dispersant. Additionally, the dispersing stability of the PPy/FAs particles in water was also found to be improved with the increase of the FA feeding ratio. Sedimentation was found in S-2 after a week. However, S-7 had been well-dispersed for more than a month as shown in Figure 3.

Spectral Analyses. Figure 4 shows the FTIR spectra of the KBr pellets of the PPy/FAs samples in the region of (4000 to 500) cm^{-1}. The spectra show a rich band fingerprint region, revealing the seven strong intensity bands. The peaks at (1540 and 1450) cm^{-1} could be attributed to the C−N and C−C asymmetric and symmetric ring stretching, respectively. Additionally, the strong peaks near (1160 and 890) cm^{-1} present the doping state of polypyrrole; the peak at 1030 cm^{-1} is attributed to the C−H deformation and N−H stretching vibrations; and the broad band at 1300 cm^{-1} demonstrates the C−H and C−N in-plane deformation vibration, respectively. All results demonstrate almost the same peak positions of the main IR bands which are associated with the structure of the PPy.[15,16] The absorbance of the −OH bands at (3352, 1323, and 1217) cm^{-1} and C═O stretching at 1710 cm^{-1} of FAs also appeared. The peak at 1380−1400 cm^{-1} is attributed to the antisymmetric COO$^-$ stretching or aliphatic C−H deformation, and the bands near 1250 cm^{-1} are attributed to the C−O stretching, O−H deformation of COOH, and the C−O stretching in phenols.[17] The strong ν(C−H) bands at (2850 and 2920) cm^{-1} and the ν(C═O) band at 1710 cm^{-1} and (1380 to 1400) cm^{-1} proved the presence of FAs in the products of the polymerizations.

UV−vis spectra of the samples were recorded in water and are given in Figure 5. The absorption spectra of samples showed a strong transition at about 280 nm corresponding to the $\pi-\pi^*$ transition band. The shift of the absorption band from (289 to 273) nm could be attributed to the polymer−solvent interaction. The nature of the solvent molecules influences the polymer chain conformation and the length of the conjugated segments, leading to a difference in the energy gaps.[18] The UV−vis spectra showed two distinct bands at 500 nm and a free tail above 800 nm in the near-infrared (NIR) region. These transitions corresponded to the transitions from the valence bond to bipolarons and antibipolarons of the oxidized form of polypyrrole. The increase in the intensity of the low-energy transition in the NIR for the PPy/FAs sample S-7 revealed that it was highly doped as compared to sample S-2. This indicated that polypyrrole had been doped by anionic FAs.

Thermal Analysis. Figure 6 shows the TGA curves of the PPy/FAs samples. It can be found that the thermal stability of the sample S-6 is better than that of the sample S-2. The weight loss relative to the PPy/FAs samples about 130 °C could be

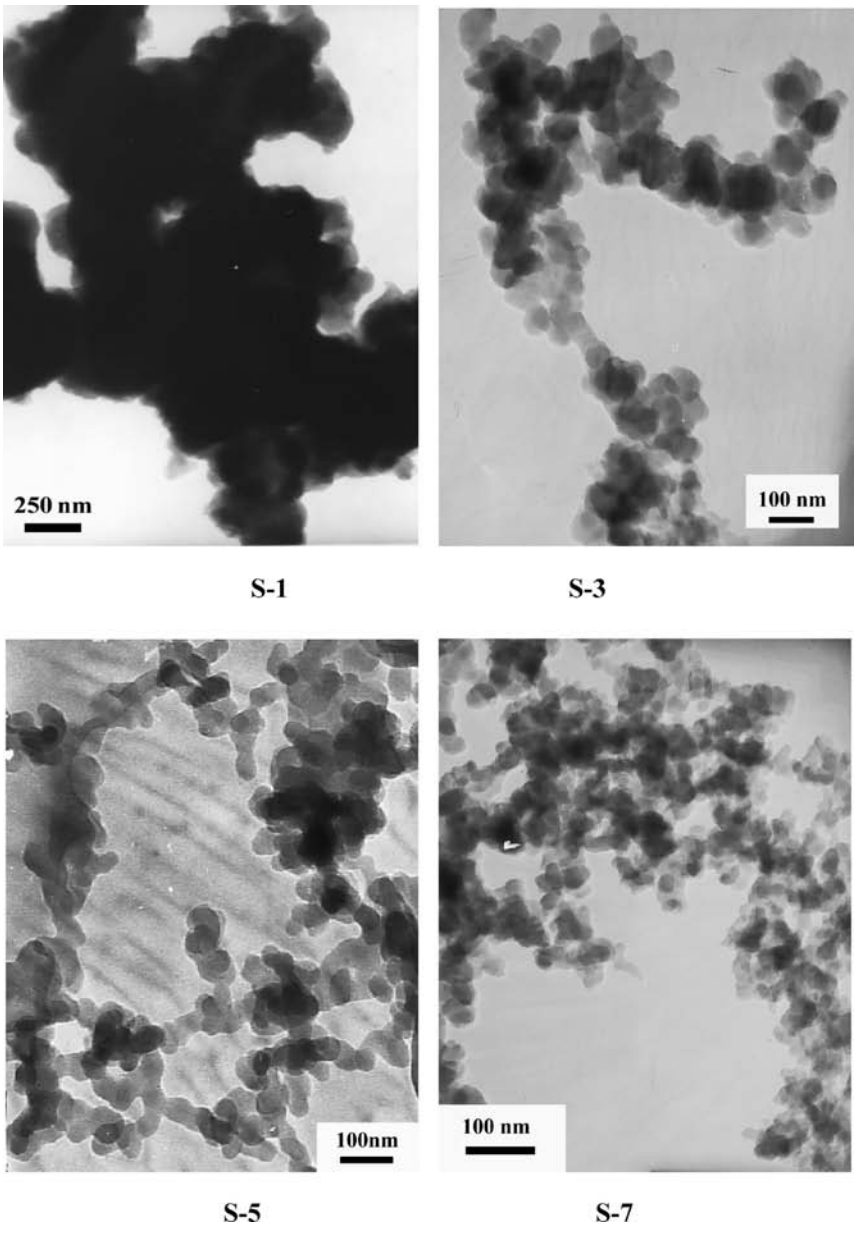

Figure 2. TEM images of the PPy/FAs samples.

indicating the hygroscopic characteristic of FAs. This may be due to the doping level of FAs which interacts with H_2O through the formation of hydrogen bonds between the carbonyls or between the carbonyls and the hydroxyl groups present in the FAs. The PPy/FAs samples begin to decompose at about 270 °C. This might result from the fact that FA is unstable. In addition, FA begins to decompose at about 250 °C. The free carboxylate groups are, in general, thermally active, and they possibly weaken the thermal degradation of the PPy composite. However, the carboxylate group becomes much more thermally stable when it forms a complex with a countercation. Thus, the TGA curves of the PPy/FAs samples clearly demonstrated the increased thermal stability on complexation of PPy with the polyelectrolyte, which in turn offers thermal processing advantages.

Electrical Conductivity. The effect of FA content on the electrical conductivity of the PPy/FAs samples is plotted in Figure 7. As for the conductivity of the different samples, a higher value of conductivity is expected when the sample has a higher doping ratio. However, the sample S-3 shows the highest conductivity though it does not give the highest value of doping ratio, which is due to the fact that the calculated doping ratio is based on the assumption that all surfactants act as dopant in the polymerization. In addition, in a system with the higher FA concentration, FAs will act as not only the dopant but also the template, and the latter effect will bring the FAs into the resulting samples due to its adsorption interaction with the polymer. In these conditions, the higher amount of surfactant anions containing bulky aliphatic chains can be a steric barrier for the charge transport in the PPy chains which results in two contrary effects on the conductivity of PPy/FAs samples.[19] Thus, we can conclude that FAs play the role of dopant as well as template, as shown in Figure 8. Additionally, FAs are not an electric conductor, and an excessive feed ratio could induce a decline of the conductivity. This may originate from the interaction between

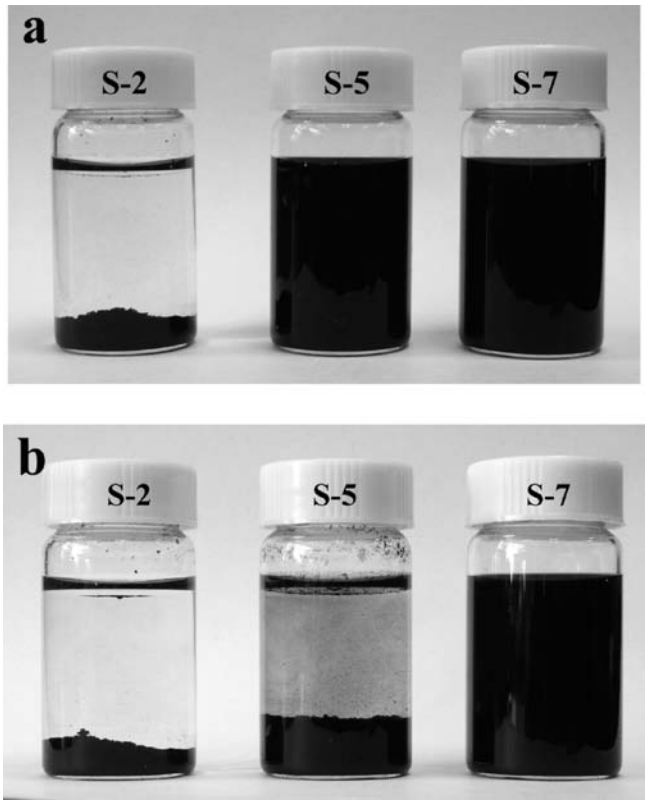

Figure 3. Water-dispersing stability of the PPy/FAs nanoparticles in water: (a) after a week and (b) after a month.

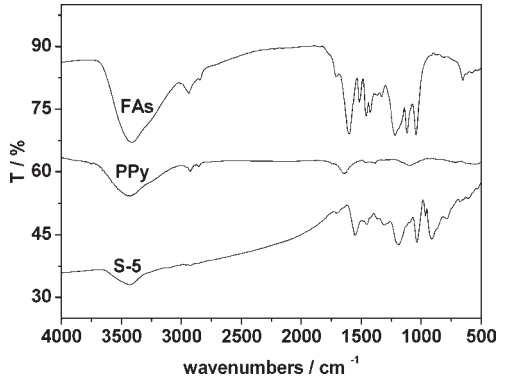

Figure 4. FTIR spectra of the KBr pellets of the PPy, FAs, and PPy/FAs nanoparticles.

APS and the polyelectrolyte. In this system, PPy doped with carboxylate is hardly yielded since the dissociation of the anionic polyelectrolyte is prevented due to the presence of the strongly electrolytic oxidant.[20]

The nanoparticles prepared by aqueous solution polymerization show a typical percolation phenomenon in terms of electrical conductivity as a function of PPy content. It has been reported that the percolation phenomenon occurs in polymer matrix-conducting composites,[21] and percolation theory was also introduced as shown in the equation followed

$$\frac{(1-\varphi)(\sigma_l^{1/t}-\sigma_m^{1/t})}{\sigma_l^{1/t}+A\sigma_m^{1/t}}+\frac{\varphi(\sigma_h^{1/t}-\sigma_m^{1/t})}{\sigma_h^{1/t}+\sigma_m^{1/t}}=0, \quad A=\frac{1-\varphi_c}{\varphi_c} \tag{1}$$

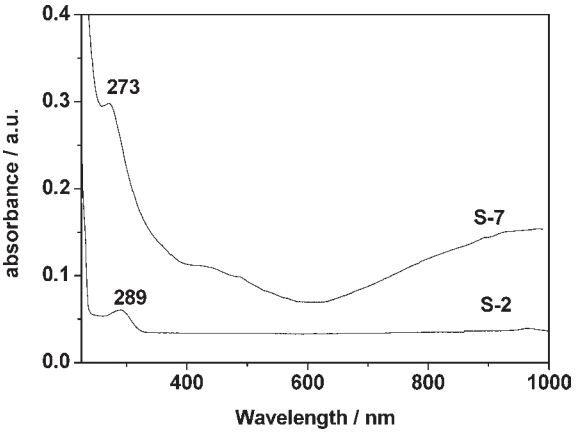

Figure 5. UV−vis absorbance spectra of the PPy/FAs samples dispersed in water.

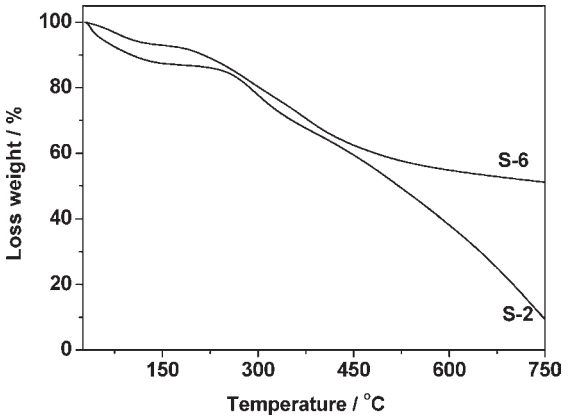

Figure 6. TGA curves of the PPy/FAs samples.

where σ_m, σ_l, and σ_h are the conductivities of the medium-, low-, and high-conductivity components, respectively. φ is the volume fraction of the high-conductivity component (PPy in this case), and φ_c is the critical concentration (i.e., percolation threshold). t is an exponent related both to the percolation threshold and to the shapes of the grains making up the medium. It is known that 0.25 to 0.30 (mole fraction) of the PPy moiety is generally doped when synthesized by chemical polymerization. Therefore, it must be assumed that the effective doping level of the PPy/FAs nanoparticles must be lower than its apparent doping level, even though the apparent doping level increased with the amount of FAs. Excessive amounts of FAs interact with PPy through the formation of hydrogen bonds between the PPy secondary amine groups and carbonyls or the hydroxyl groups present in the FAs.

Temperature Dependence of the Electrical Conductivity. The temperature dependence of the conductivity for the PPy/FAs samples is presented in Figure 9. As the temperature increases, the conductivity increases from (283 to 423) K. This figure clearly indicates that, despite the rather similar sample preparation conditions, the temperature dependences of the conductivity show all the samples had a semiconducting property. For semiconductors, the higher the temperature, the higher the electrical conductivity. However, the samples which are in the low contents of FAs have a strongly temperature-dependent conductivity over the entire temperature interval from (283 to 423) K. It is worth noticing that samples that are in the high content of FAs

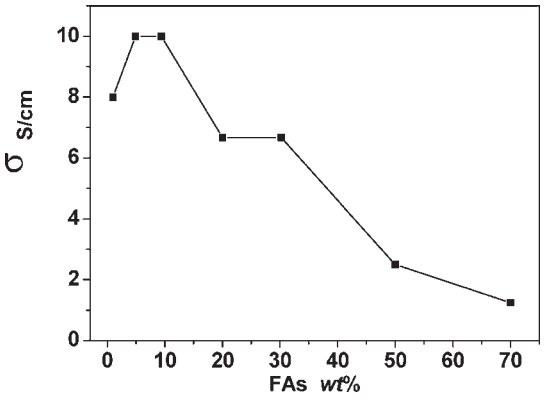

Figure 7. Electrical conductivities of the PPy/FAs samples at room temperature.

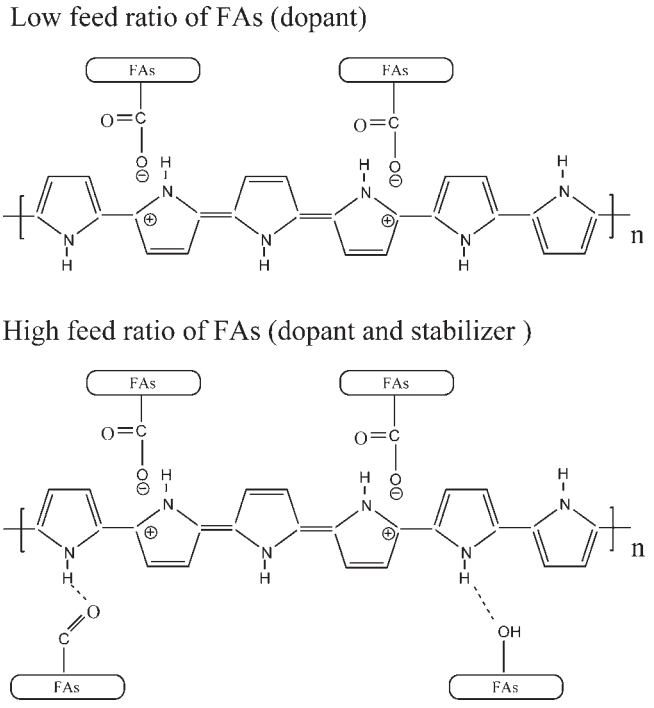

Figure 8. Proposed schematic for the polymerization of pyrrole in the presence of FAs.

have a weakly temperature-dependent conductivity. The inherent disordered nature is found in semiconducting polymers like polypyrrole. Thus, the temperature dependence of conductivity $\sigma(T)$ can be described by the Mott's variable range hopping (VRH) model[22]

$$\sigma(T) = \sigma_o \exp[-(T_o/T)^{\gamma}] \quad (2)$$

where σ_o is the high-temperature limit of conductivity and T_0 is Mott's characteristic temperature associated with the degree of localization of the electronic wave function. The exponent $\gamma = 1/(1 + d)$ determines the dimensionality of the conducting medium. The possible values of γ are 1/4, 1/3, and 1/2 for three-, two-, and one-dimensional systems, respectively. The best fitted value of γ is obtained by the linear regression analysis. The lowest standard deviations are found for γ = 1/4 for S-2, S-4, and S-7, respectively. The linear dependence of ln σ on $T^{-1/4}$, as shown

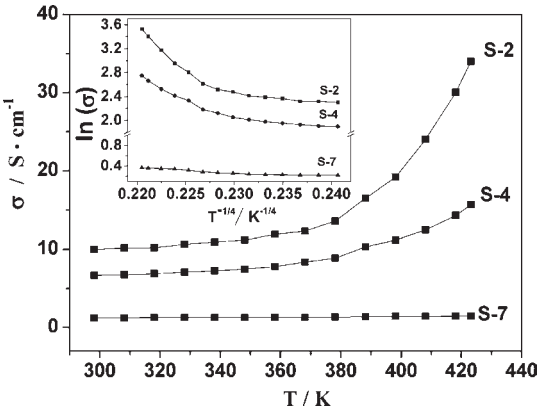

Figure 9. Temperature dependence of electrical conductivity of the PPy/FAs samples.

Table 2. Parameters σ_o and T_o as Defined in Equation 2, Density of States Hopping Length R_{hop}, and Activation Energy W_{hop}

	σ_o	T_o	R_{283K}	W_{283K}	R_{423K}	W_{423K}
sample	S·cm^{-1}	K	Å	meV	Å	meV
S-2	7060313	10547114	15.6	84.7	14.1	109.6
S-4	115844	2883821	11.3	61.3	10.2	82.9
S-7	8	4269	2.2	12.0	2.0	16.3

in Figure 9, indicates that three-dimensional (3D) charge transport occurs in the PPy/FAs samples. The values of Mott's characteristic temperature T_o and the pre-exponential factor σ_o are obtained from the slopes and intercepts of Figure 9 and are given in Table 2. The values of T_o and σ_o decrease with increasing FA content. The average hopping distance R_{hop} between two sites and the activation energy W_{hop} are

$$R_{hop} = (3/8)(T_o/T)^{1/4}L \quad (3)$$

$$W_{hop} = (1/4)kT(T_o/T)^{1/4} \quad (4)$$

where L is the localization length of the PPy phase, assuming the localization length of the pyrrole monomer unit is about 3 Å.[23]

At room temperature, the average hopping distances for sample S-2, S-4, and S-7 were about 15.6 Å, 11.3 Å, and 2.2 Å, and it reduces to about 14.1 Å, 10.2 Å, and 2 Å for content variation of PPy. The estimated activation energies for hopping as shown in Table 2 are in the range of 109.6 meV to 12 meV. This implied that the decrease in hopping distance and hopping energy enhanced the stability of conductivity when temperature changed.

CONCLUSIONS

In summary, we utilized a renewable resource fulvic acid which was a natural hydrophilic polymer with a vast number of hydroxyl and carboxyl groups as both the stabilizer and the dopant for the water-dispersed and weak temperature-dependent polypyrrole nanoparticles. For the first time, the aggregation of the pyrrole/FAs samples has been systematically controlled to tune the properties of polypyrrole. The present approach has many advantages: (i) renewable resource anionic FAs were utilized as the structure-directing agents for tuning the properties of polypyrrole

dx.doi.org/10.1021/je100751n |J. Chem. Eng. Data 2011, 56, 899–904

nanoparticles; (ii) the PPy/FAs nanoparticles are weakly temperature dependent on electrical conductivity over the entire temperature interval from (283 to 423) K, which is very rarely reported in the literature; and (iii) the FAs are very cheap and can be easily obtained from both soils and municipal waste composites.

AUTHOR INFORMATION

Corresponding Author

*Tel.: +86 931 8912516. Fax: +86 931 8912582. E-mail: pliu@lzu.edu.cn.

REFERENCES

(1) Intelmann, C. M.; Syritski, V.; Tsankov, D.; Hinrichs, K.; Rappich, J. Ultrathin polypyrrole films on silicon substrates. *Electrochim. Acta* **2008**, *53*, 4046.

(2) Bengoechea, M.; Boyano, I.; Miguel, O.; Cantero, I.; Ochoteco, E.; Pomposo, J.; Grande, H. Chemical reduction method for industrial application of undoped polypyrrole electrodes in lithium-ion batteries. *J. Power Sources* **2006**, *160*, 585–591.

(3) Reut, J.; Opik, A.; Idla, K. Corrosion behavior of polypyrrole coated mild steel. *Synth. Met.* **1999**, *102*, 1392–1393.

(4) Pomposo, J. A.; Rodriguez, J.; Grande, H. Polypyrrole-based conducting hot melt adhesives for EMI shielding applications. *Synth. Met.* **1999**, *104*, 107–111.

(5) Ren, X.; Zhao, Q.; Liu, J.; Liang, X.; Zhang, Q.; Zhang, P. Preparation of polypyrrole nanoparticles in reverse micelle and its application to glucose biosensor. *J. Nanosci. Nanotechnol.* **2008**, *8*, 2643–2646.

(6) Berdichevsky, Y.; Lo, Y. H. Polypyrrole nanowire actuators. *Adv. Mater.* **2006**, *18*, 122–125.

(7) Ramanaviciene, A.; Ramanavicius, A. Molecularly imprinted polypyrrole-based synthetic receptor for direct detection of bovine leukemia virus glycoproteins. *Biosens. Bioelectron.* **2004**, *20*, 1076–1082.

(8) Göran, F.; Aamir, R.; Kristina, G.; Leif, N.; Albert, M. Ionic Motion in Polypyrrole-Cellulose Composites: Trap Release Mechanism during Potentiostatic Reduction. *J. Phys. Chem. B* **2009**, *113*, 4582–4589.

(9) Yang, C.; Liu, P. Water-Dispersed Conductive Polypyrroles Doped with Lignosulfonate and the Weak Temperature Dependence of Electrical Conductivity. *Ind. Eng. Chem. Res.* **2009**, *48*, 9498–9503.

(10) Alvarez-Puebla, R. A.; Valenzuela-Calahorro, C.; Garrido, J. J. Theoretical study on fulvic acid structure, conformation and aggregation-a molecular modelling approach. *Sci. Total Environ.* **2006**, *358*, 243–254.

(11) García-Gil, J. C.; Plaza, C.; Fernández, J. M.; Senesi, N.; Polo, A. Soil fulvic acid characteristics and proton binding behavior as affected by long-term municipal waste compost amendment under semi-arid environment. *Geoderma* **2008**, *146*, 363–369.

(12) Bolto, B. A. Soluble Polymers in Water Purification. *Prog. Polym. Sci.* **1995**, *20*, 987–1041.

(13) Dos Santos, D. D., Jr.; Alvarez-Puebla, R. A.; Oliveira, O. N., Jr.; Aroca, R. F. Controlling the size and shape of gold nanoparticles in fulvic acid colloidal solutions and their optical characterization using SERS. *J. Mater. Chem.* **2005**, *15*, 3045–3049.

(14) Liu, Y. Q.; Gao, L.; Zheng, S.; Wang, Y.; Sun, J.; Kajiura, H.; Li, Y. M.; Noda, K. Dubundling of single-walled carbon nanotubes by using natural polyeletrolytes. *Nanotechnology* **2007**, *18*, 365702.

(15) Aguilar-Hernandez, J.; Potje-Kamloth, K. Optical and electrical characterization of a conducting polypyrrole composite prepared by insitu electropolymerization. *Phys. Chem. Chem. Phys.* **1999**, *1*, 1735–1742.

(16) Geng, L.; Wang, S.; Zhao, Y.; Li, P.; Zhang, S.; Huang, W.; Wu, S. Study of the primary sensitivity of polypyrrole/γ-Fe_2O_3 to toxic gases. *Mater. Chem. Phys.* **2006**, *99*, 15–19.

(17) Fu, H.; Quan, X. Complexes of fulvic acid on the surface of hematite, goethite, and akaganeite: FTIR observation. *Chemosphere* **2006**, *63*, 403–410.

(18) Brédas, J. L. In *Electronic Properties of Polymers and Related Conpounds*; Springer: New York, 1985.

(19) Omastova, M.; Trchova, M.; Pionteck, J.; Prokes, J.; Stejskal, J. Effect of polymerization conditions on the properties of polypyrrole prepared in the presence of sodium bis(2-ethylhexyl) sulfosuccinate. *Synth. Met.* **2004**, *143*, 153–161.

(20) Kudoh, Y. Properties of polypyrrole prepared by chemical polymerization using aqueous solution containing $Fe_2(SO_4)_3$ and anionic surfactant. *Synth. Met.* **1996**, *79*, 17–22.

(21) Carrasco, P. M.; Grande, H. J.; Cortazar, M.; Alberdi, J. M. Structure-conductivity relationships in chemical polypyrroles of low, medium and high conductivity. *Synth. Met.* **2006**, *156*, 420–425.

(22) Yoshimoto, S.; Ohashi, F.; Kameyama, T. Insertion of Polypyrrole Chains into Montmorillonite Galleries by a Solvent-Free Mechanochemical Route. *Macromol. Rapid Commun.* **2005**, *26*, 461–466.

(23) Dutta, K.; De, S. K. Optical and diode like current-voltage characteristics of SnO2-polypyrrole nanocomposites. *J. Phys. D: Appl. Phys.* **2007**, *40*, 734–739.